High Energy Astroparticle Physics (Astronomy?) with H.E.S.S.

Rafał Moderski
Nicolaus Copernicus Astronomical Center

H.E.S.S. - basic data

– **High Energy Stereoscopic System**;
– **five telescopes** 120 m x 120 m area;
– **4x13 m** diameter spherical main mirror f=13 m, 362 circular mirror facets 60 cm diameter, 4 x 107m^2 collecting area, camera: 960 vacuum tube photo-multipliers, field of view ~5°; 1ns sampling;
– **1x28 m** diameter parabolic mirror f=36 m, 614 m^2 area, 875 hexagonal mirror facets 90 cm (flat-to-flat), camera: 2048 photo-multipliers, 1 ns sampling, field of view ~3.2°, 2.8 t
– duty cycle ~1000h/yr (moonless nights required);
– energy range: **~30GeV - >10TeV**
– resolution: **angular – 0.1°, energetic – 15% @ 1TeV**
– sensitivity: **1% Crab** (5σ, 25h)

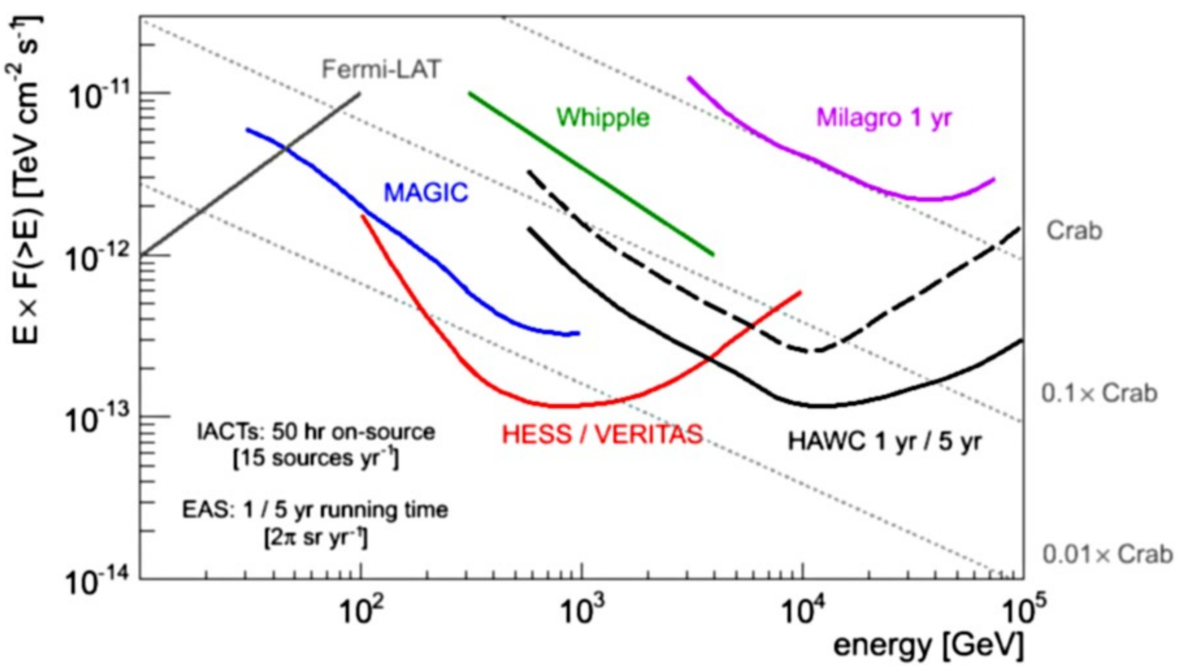

HESS Collaboration

>12 countries, >30 scientific institutions, >100 scientists

Max-Planck-Institut für Kernphysik, Heidelberg, Germany
Humboldt Universität Berlin, Germany, Institut für Physik
Ruhr-Universität Bochum, Germany, Fakultät für Physik und Astronomie
Universität Erlangen-Nürnberg, Germany, Physikalisches Institut
Universität Hamburg, Germany, II. Institut für Experimentalphysik
Landessternwarte Heidelberg, Germany
Universität Tübingen, Germany, Institut für Astronomie und Astrophysik (IAAT)
Laboratoire Leprince-Ringuet (LLR), Ecole Polytechnique, Palaiseau, France
LPNHE, Universités Paris VI - VII, France,
APC, Paris, France
CEA Saclay, France
Observatoire de Paris-Meudon, DAEC, France
LAPP Annecy, France
Université de Grenoble, France
LPTA, Université Montpellier II, France
CERS, Toulouse, France
Durham University, U.K.
University of Leeds, School of Physics and Astronomy
Dublin Institute for Advanced Studies, Dublin, Ireland

Nicolaus Copernicus Astronomical Center, Polish Academy of Sciences, Warsaw, Poland
J. Dyks, W. Kluźniak, R. Moderski, B. Rudak, A. Zdziarski
Astronomical Observatory, Jagiellonian University, Cracow, Poland
M. Ostrowski, Ł.Stawarz
Institute of Nuclear Physics, Polish Academy of Sciences, Cracow, Poland
J. Niemiec, M. Dyrda
Astronomical Observatory, University of Warsaw, Poland
T. Bulik
Center for Astronomy, Nicolaus Copernicus University, Toruń, Poland
K. Katarzyński

Charles University, Prag, Czech Republic, Nuclear Center
Yerevan Physics Institute, Yerevan, Armenia
University of Adelaide, Australia, School of Chemistry and Physics
University of Namibia, Windhoek, Namibia
North West University, Republic of South Africa

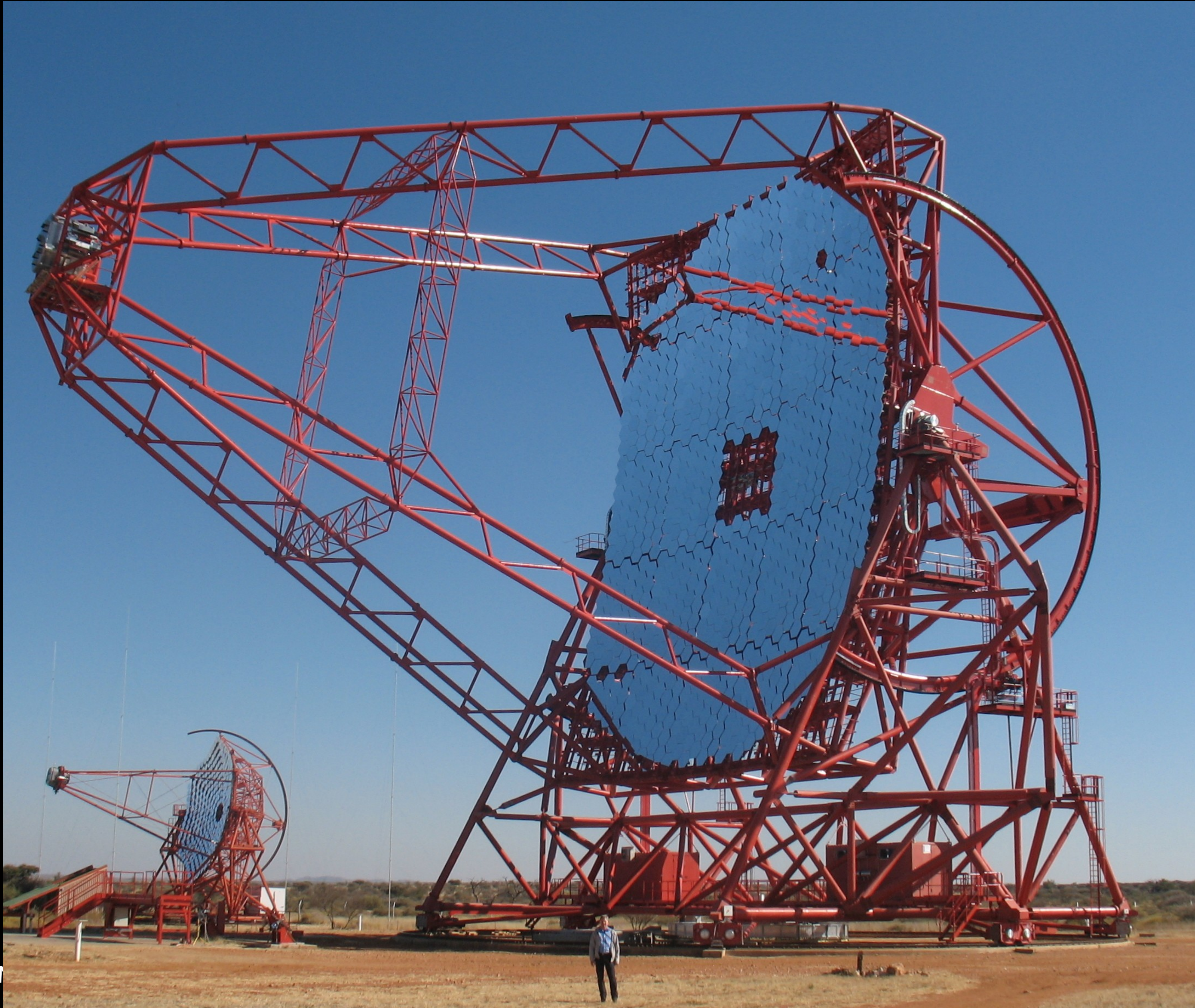

weight: 580t
height of elevation axis: 24m
mirror dimensions: 32,6m x 24,4m
focal length: 36m (total height: 60m)
slew speed: 100°/min

Cherenkov technique

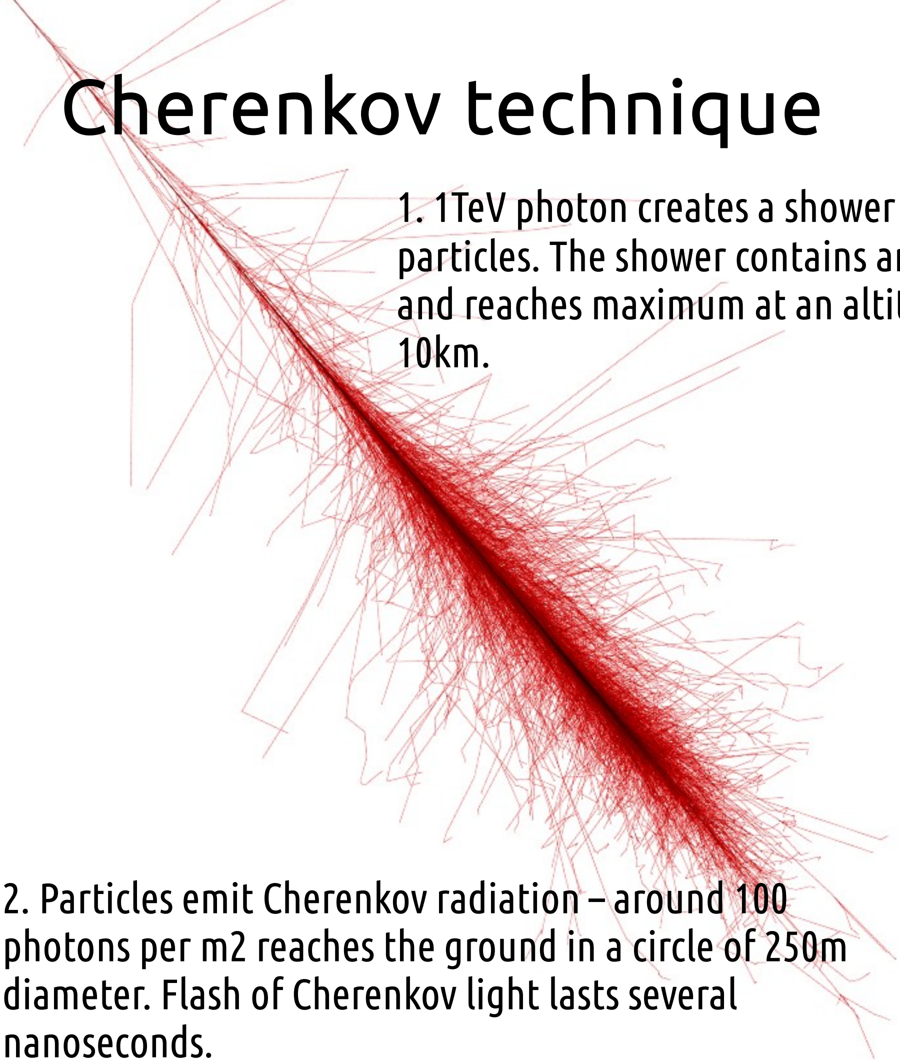

1. 1TeV photon creates a shower of secondary particles. The shower contains around 10^5 e^+e^- pairs and reaches maximum at an altitude of around 10km.

2. Particles emit Cherenkov radiation – around 100 photons per m2 reaches the ground in a circle of 250m diameter. Flash of Cherenkov light lasts several nanoseconds.

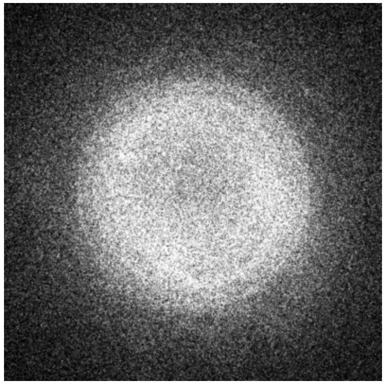

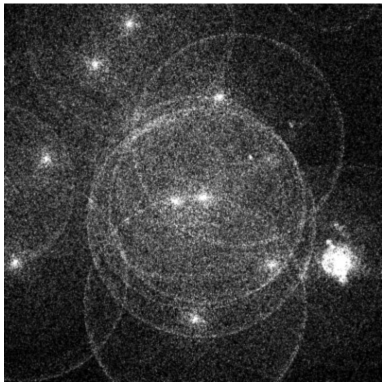

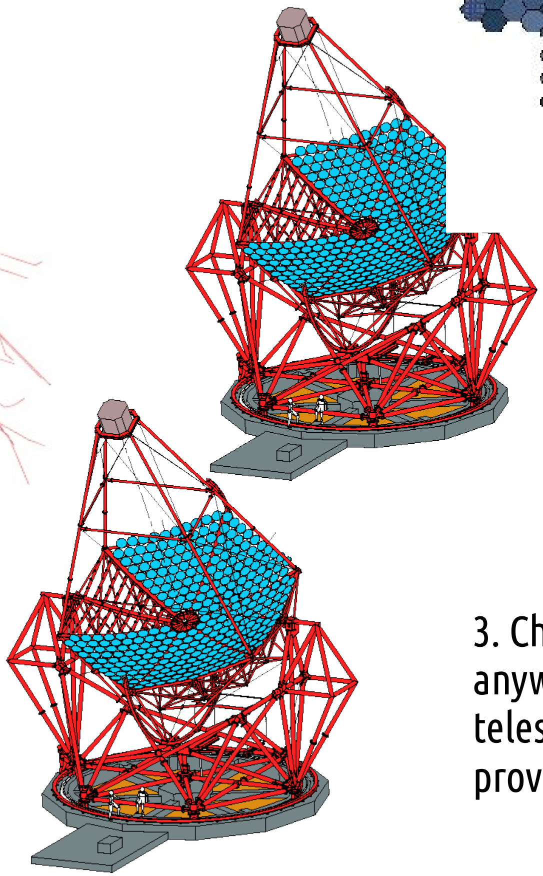

3. Cherenkov photons can be registered anywhere within the cone by an optical telescope (if enough sensitive) – this provides an effective area of **50000m^2**

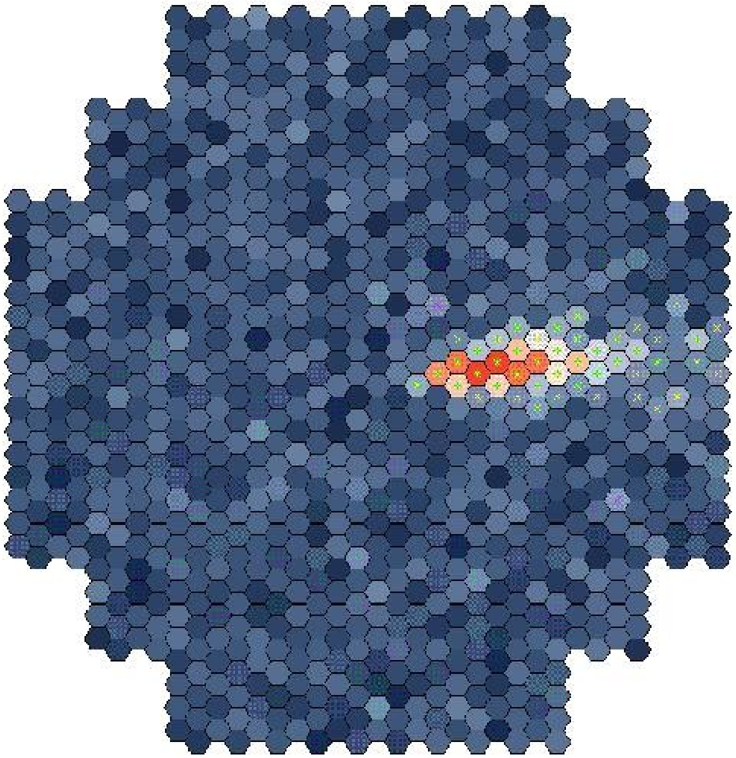

4. Image of the air shower is captured by the camera.

Cherenkov technique - stereoscopy

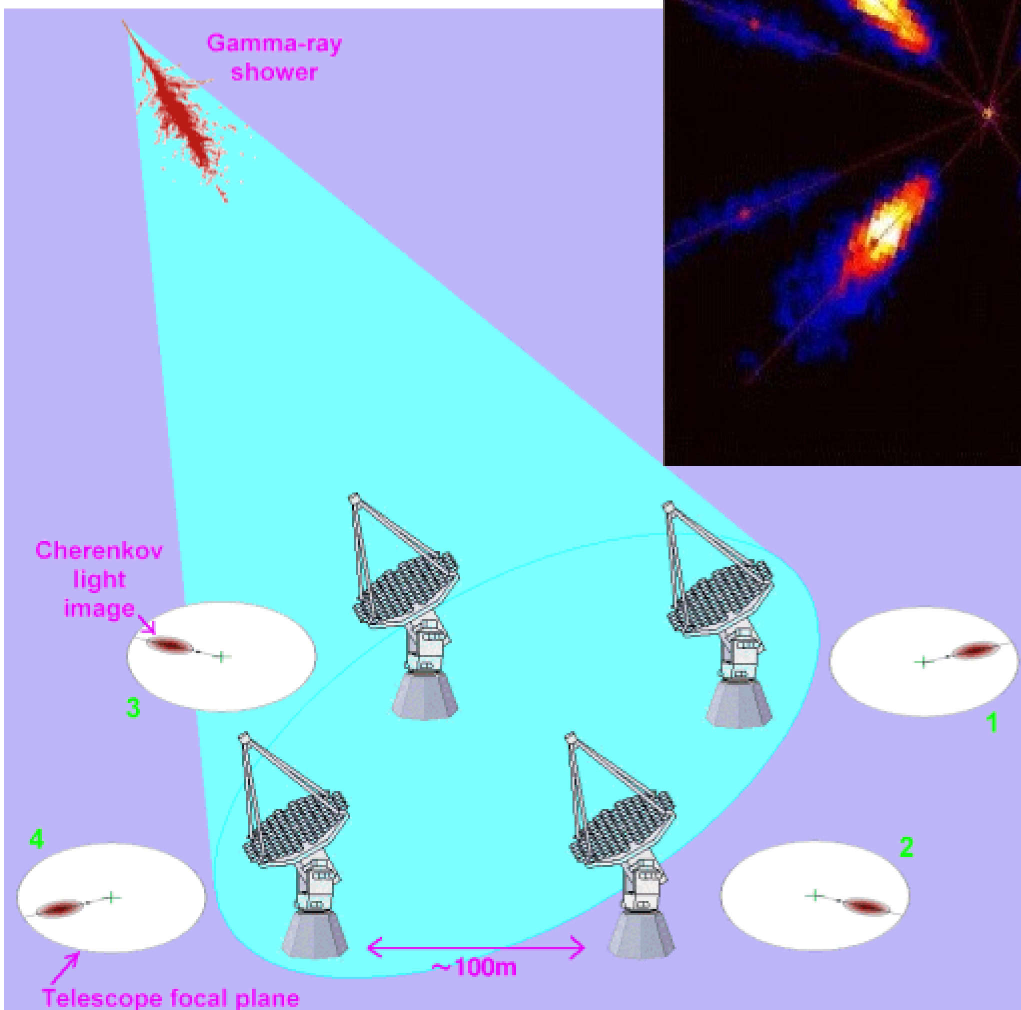

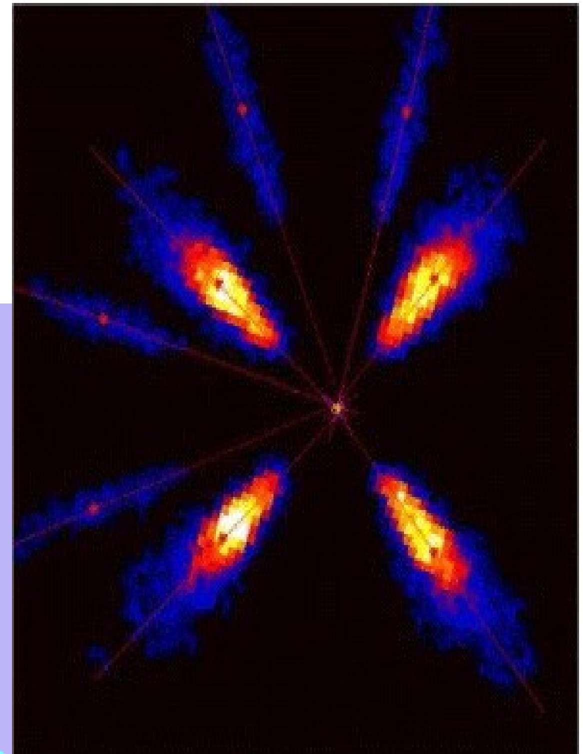

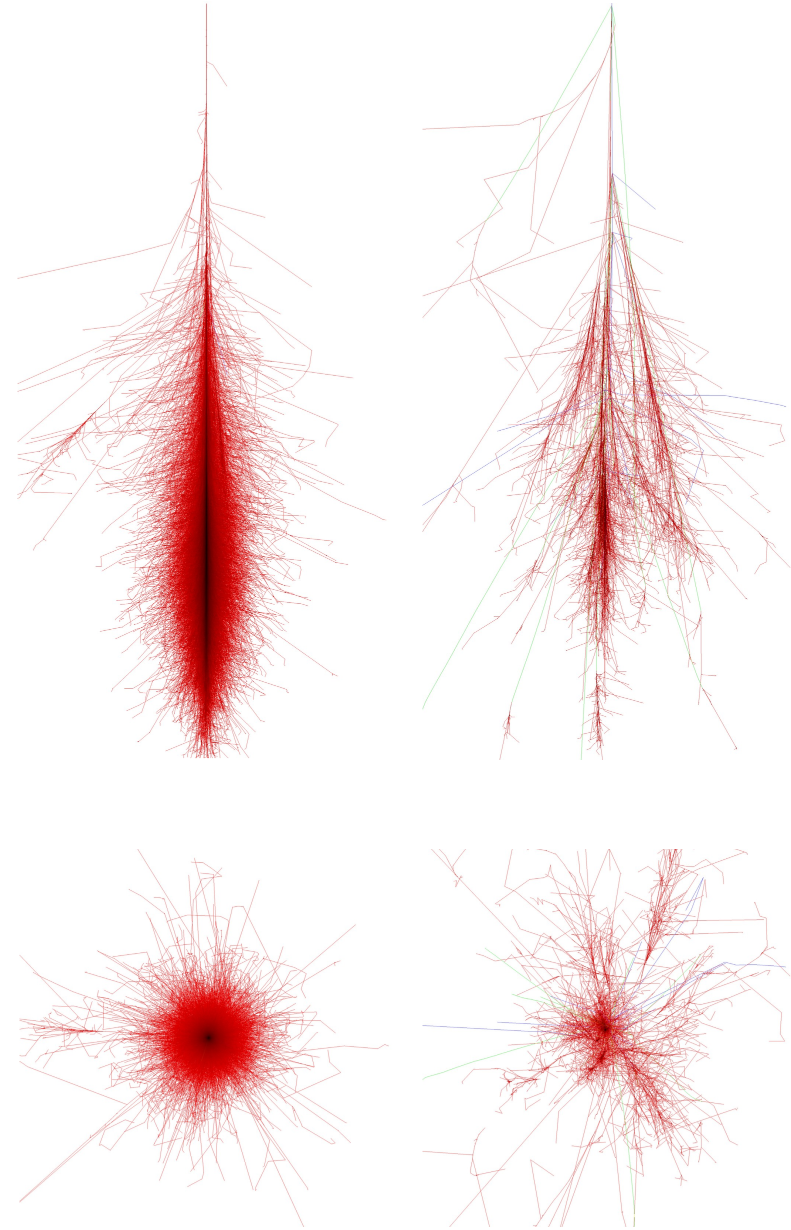

Astroparticle research

Galactic sources:

- supernova remnants (SNRs),
- pulsars and pulsar wind nebulae (PWNs),
- star clusters,
- Galactic centre,
- X-ray binaries (XRBs) and microquasars.

Extragalactic sources:

- active galactic nuclei (AGNs),
- dwarf galaxies (DSs),
- extragalactic background light (EBL),
- gamma-ray bursts (GRBs),
- clusters of galaxies.

Fundamental physics:

- dark matter (DM),
- Lorentz invariance violation (LIV),
- cosmic-rays (CR).

Physical processes:

- particle acceleration to the highest energies,
- particle and radiation propagation in the intergalactic medium,
- structure of the magnetic field at different scales,
- radiation production mechanisms at high energy.

H.E.S.S. - some results

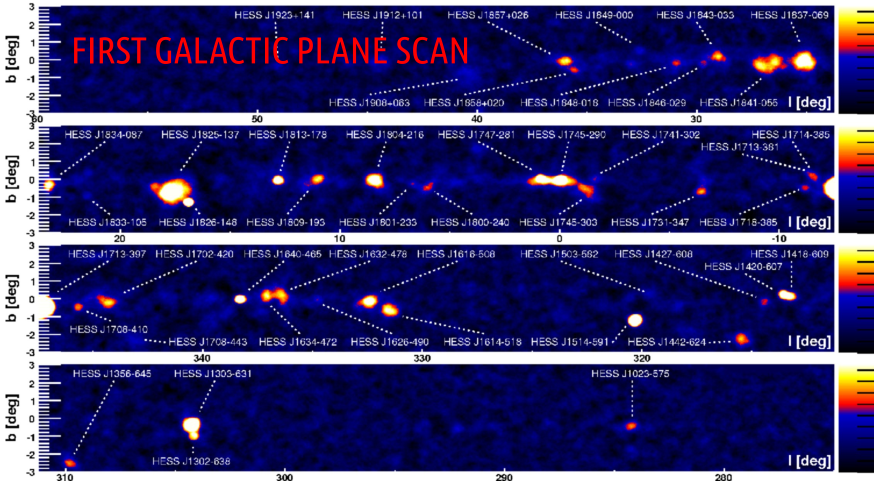

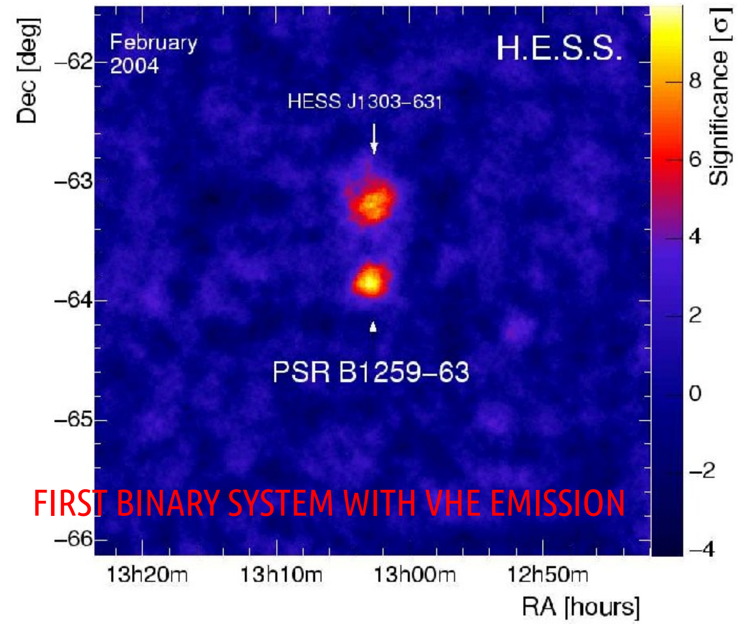

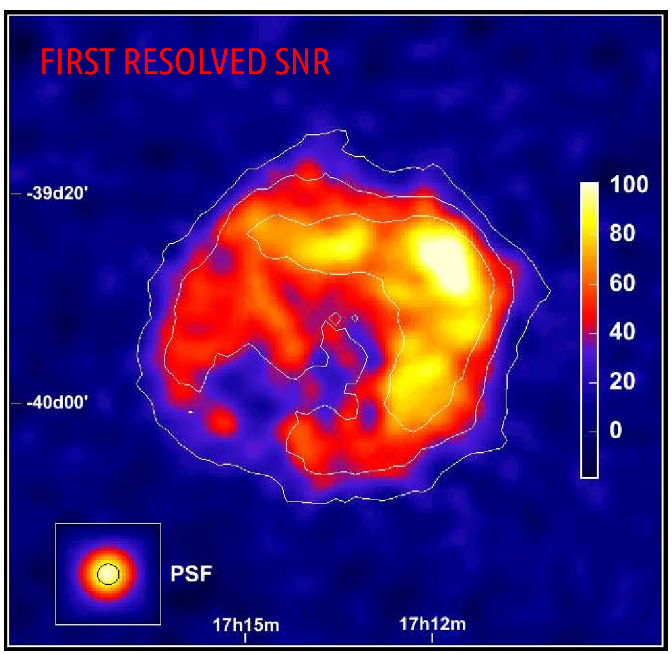

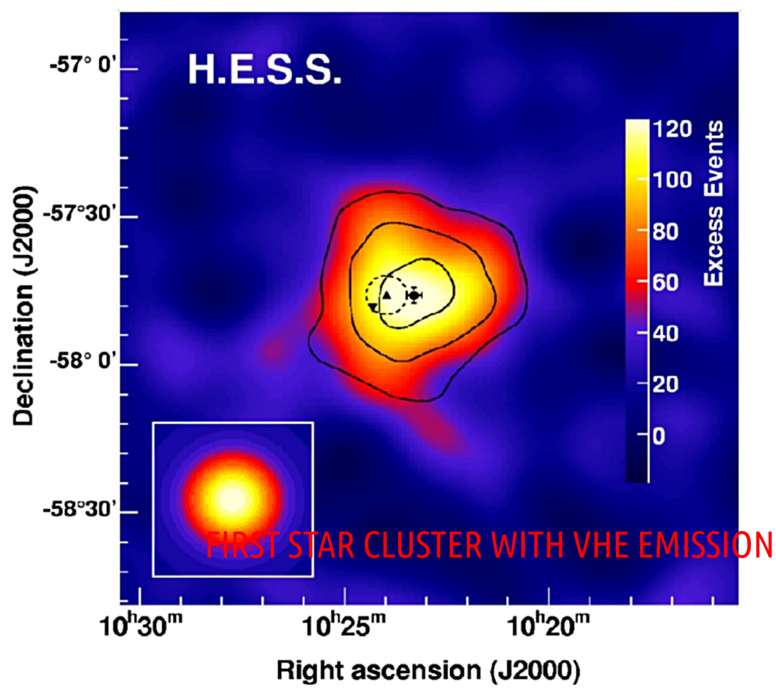

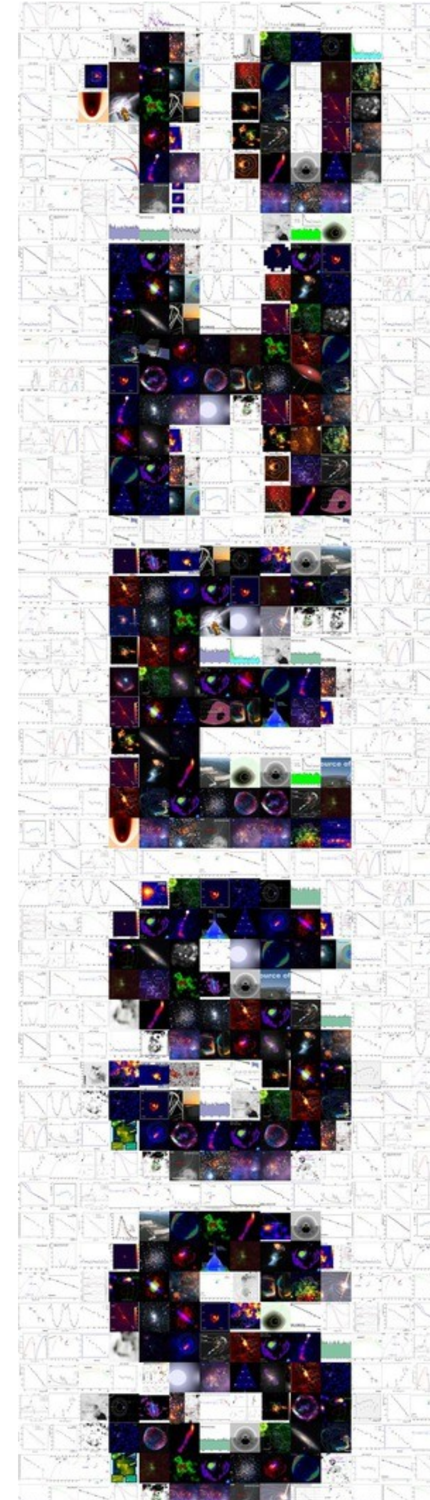

Vela pulsar with H.E.S.S. II

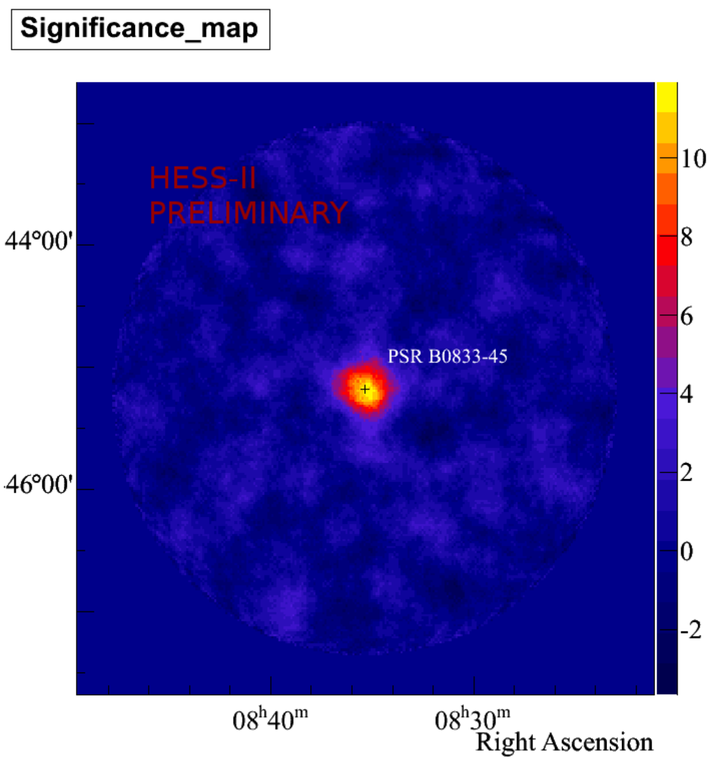

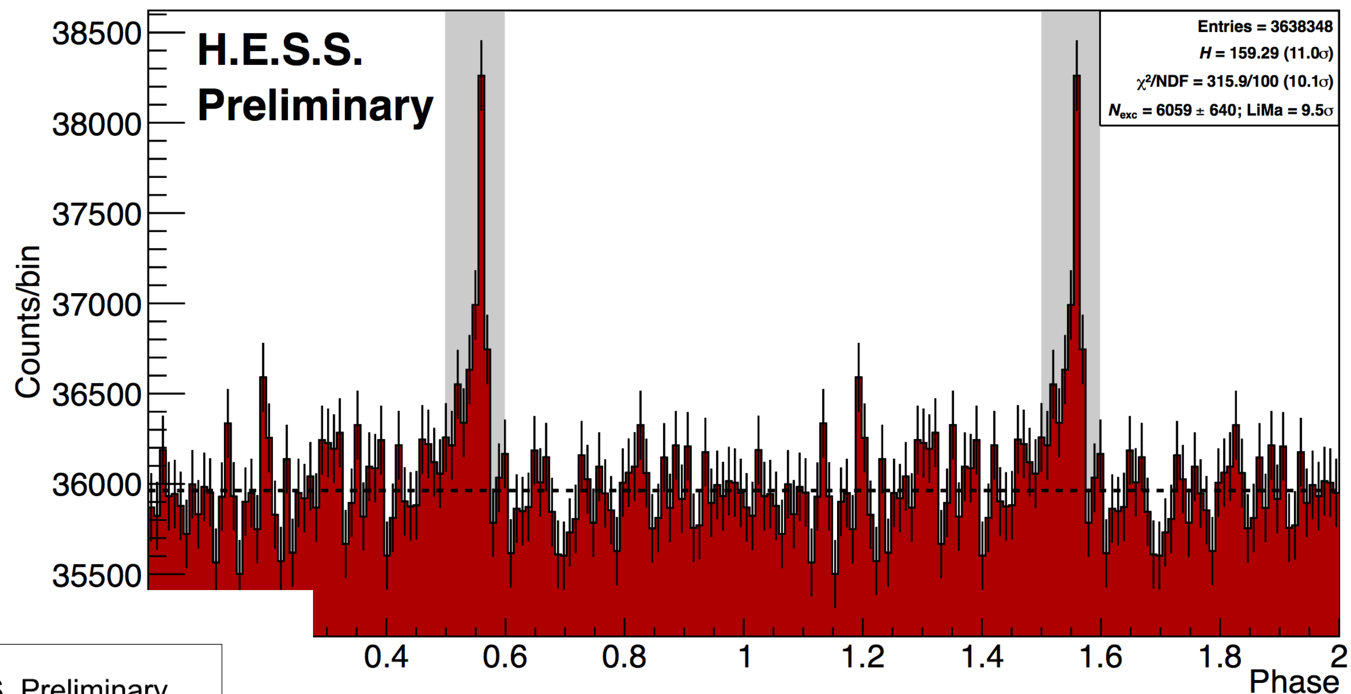

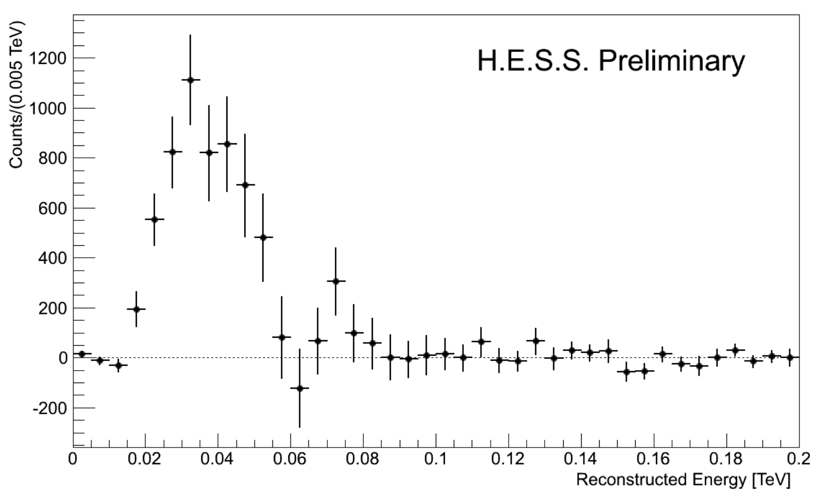

Galactic Plane Scan

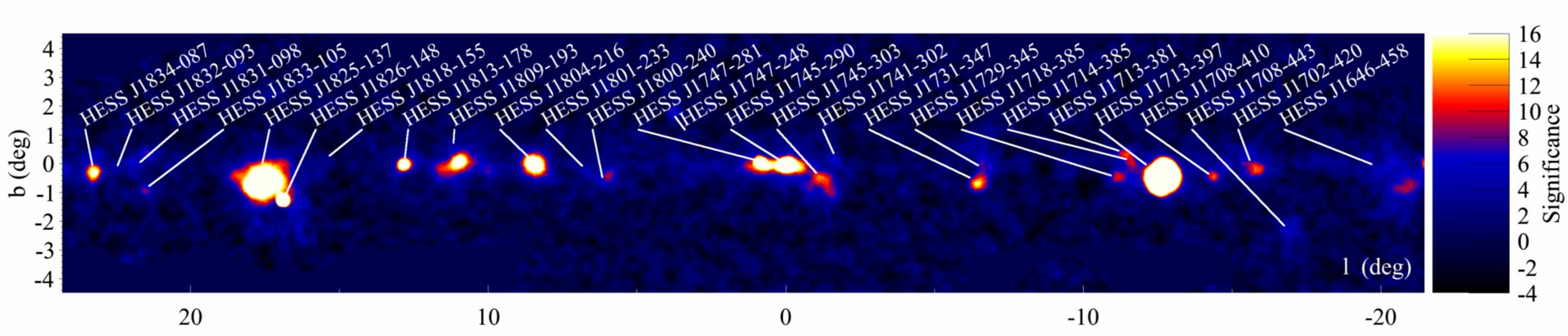

– survey of +/- 3^{o} lat and 250^{o}-70^{o} long
– over 2350h exposure
– over 50 sources (79 in official H.E.S.S. catalog including extragalactic

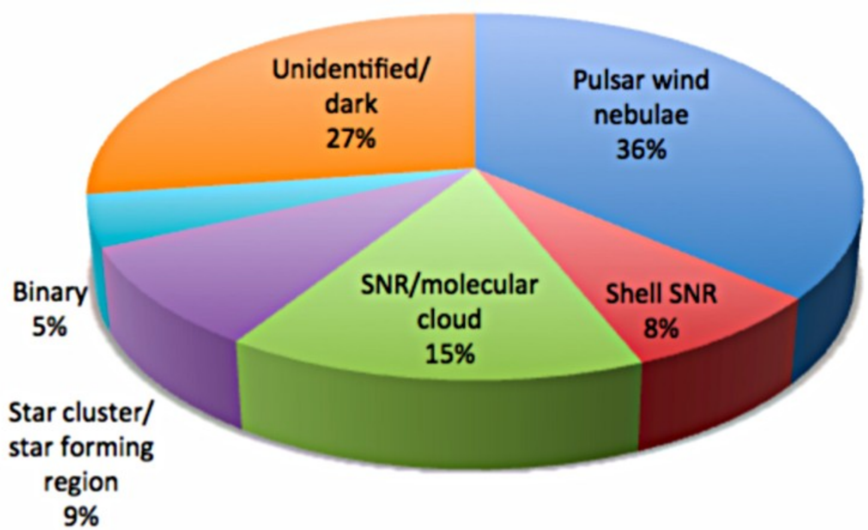

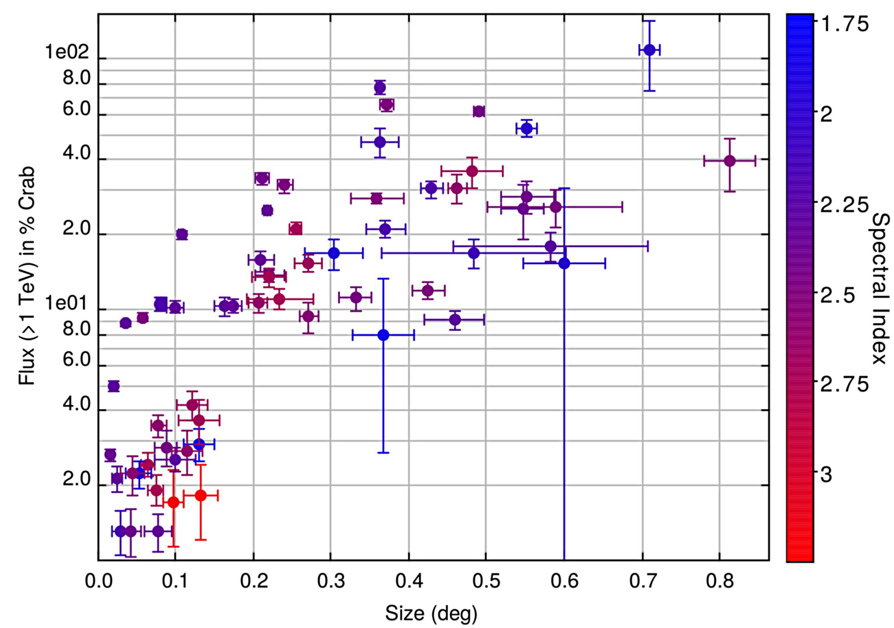

Fig. 17. Size – flux scatter plot for the sources in the HGPS, with spectral index shown in color. The size-dependent sensitivity of the survey is clearly visible; the detection threshold is higher at higher flux for larger sources. The fact that there are no sources in the upper left corner is not a selection effect, a source located there would have been detected.

Sources in the Large Magellanic Cloud

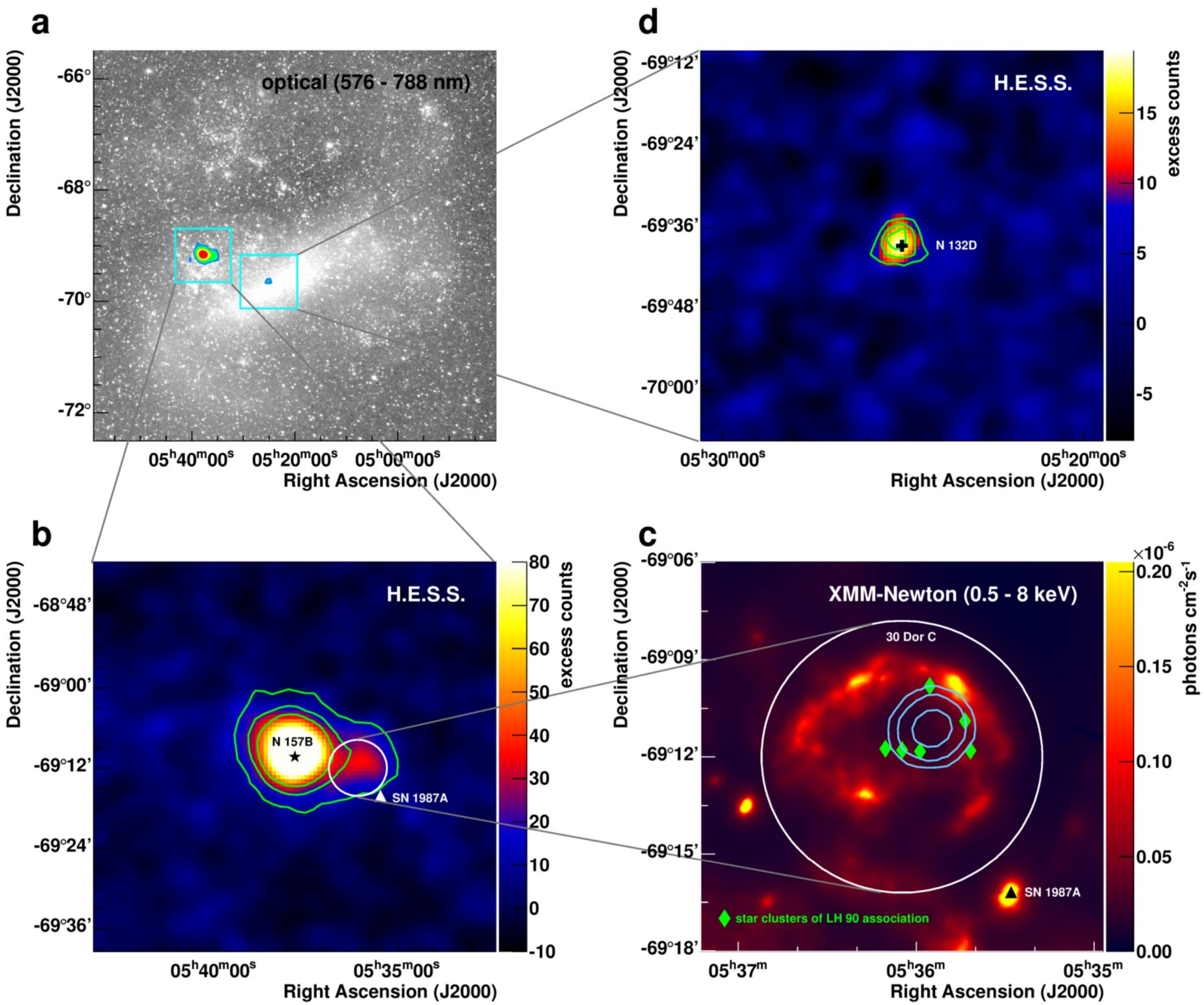

– LMC – 4% of the Milky Way mass; 50kpc distance; detected by Fermi but sources not resolved; high star formation rate, numerous massive star clusters and SNRs (e.g. SN1987A)

– 210h exposure; three sources detected: pulsar wind nebula PWN N 157B, superbubble 30 Dor C, and supernova remnant SNR N 132D

– no signal from SN1987A

Sources in the Large Magellanic Cloud

PWN N 157B

– nebula of ultrarelativistic particles driven by a pulsar PSR J0537-6910 (twin of the Crab pulsar – 4.9 x 10^{38} erg s^{-1})

– but smaller magnetic field - 45uG vs. 124 uG

– VHE emission due to IC of infrared radiation field form nearby LH99 star cluster

30 Dor C

– VHE emission from interaction of CRs with interstellar medium (pion production) or from IC upscattering of low energy photons by the same population of electrons which are responsible for the X-ray synchrotron radiation,

– right conditions to accelerate some protons to energies exceeding 3 x 10^{15} eV

SNR N 132D

– old SNR ~6000 yr

– its age lies in the gap between young (< 2000 yr) TeV-emitting SNRs, and old (>10000 yr) TeV-quiet SNRs - an indication of how long SNRs contain CRs with energies in excess of 10^{13} eV

First AGNs detected by H.E.S.S. II (mono)

PG 1553+113

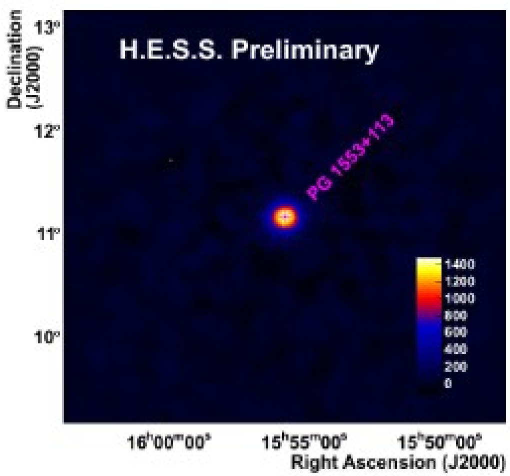

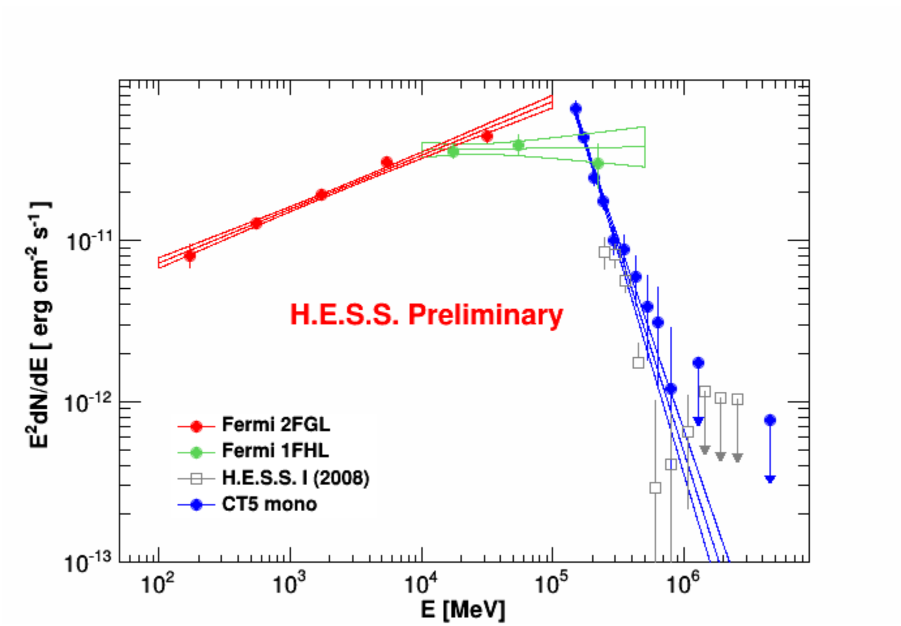

PKS 2155-304

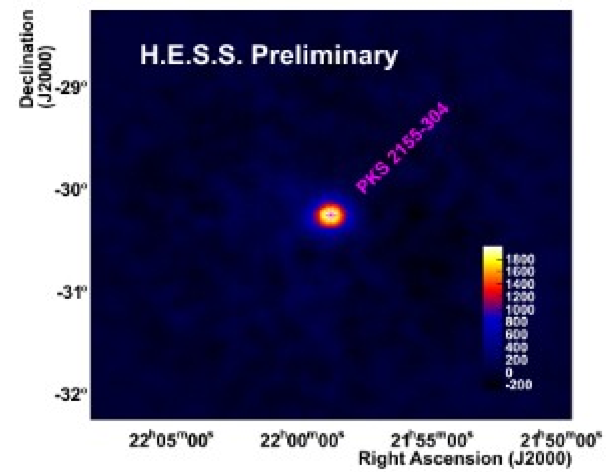

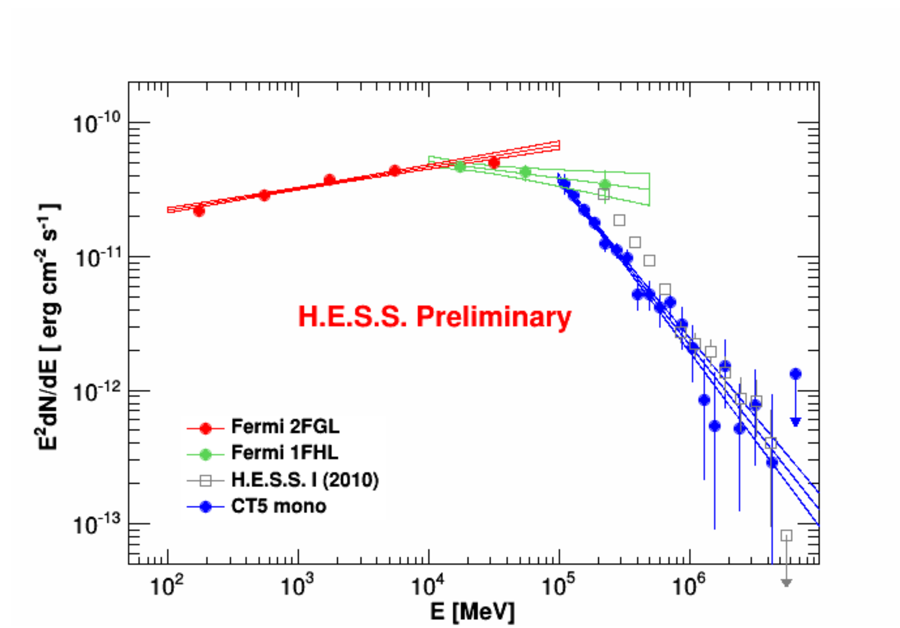

First AGNs detected by H.E.S.S. II

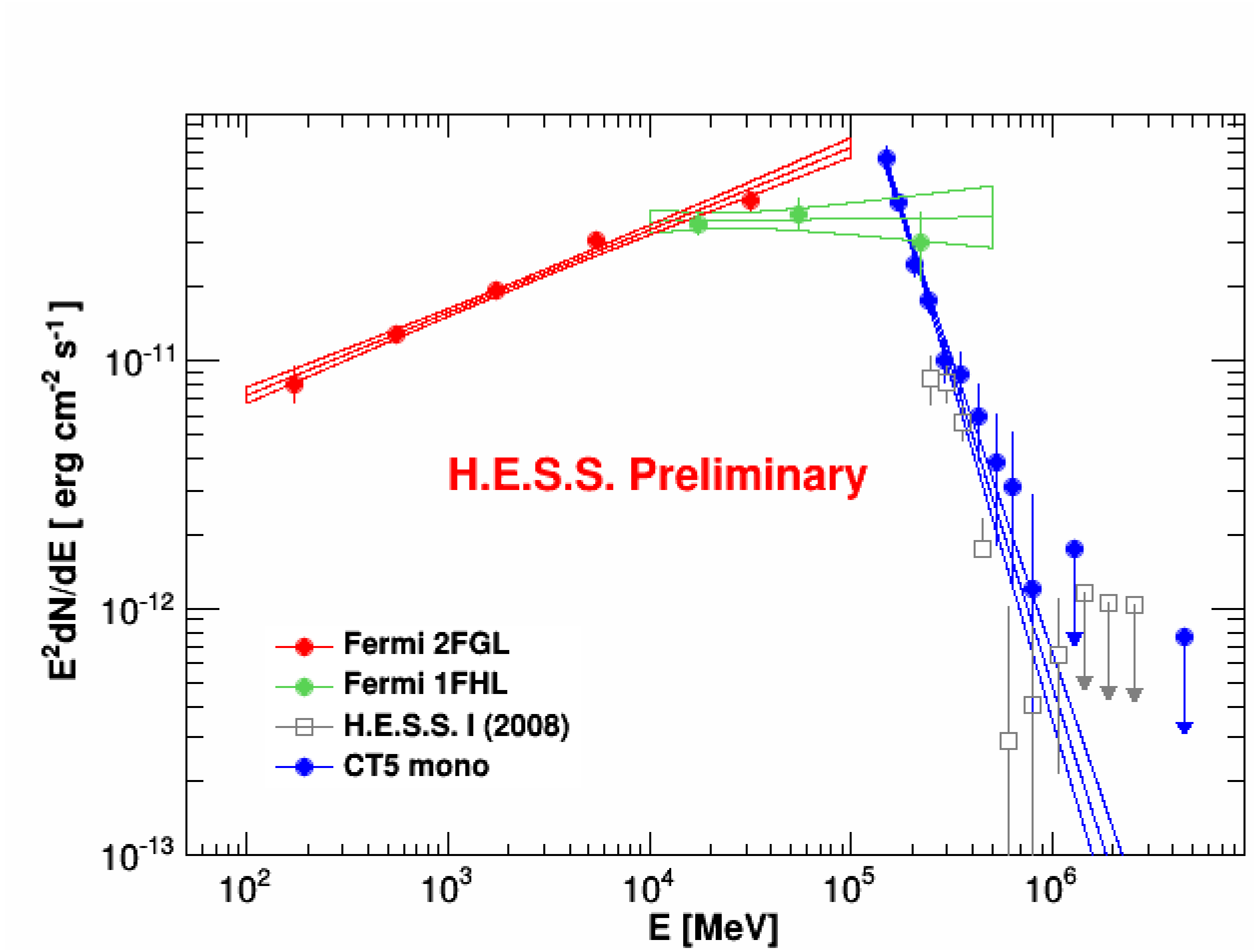

Extragalactic background light

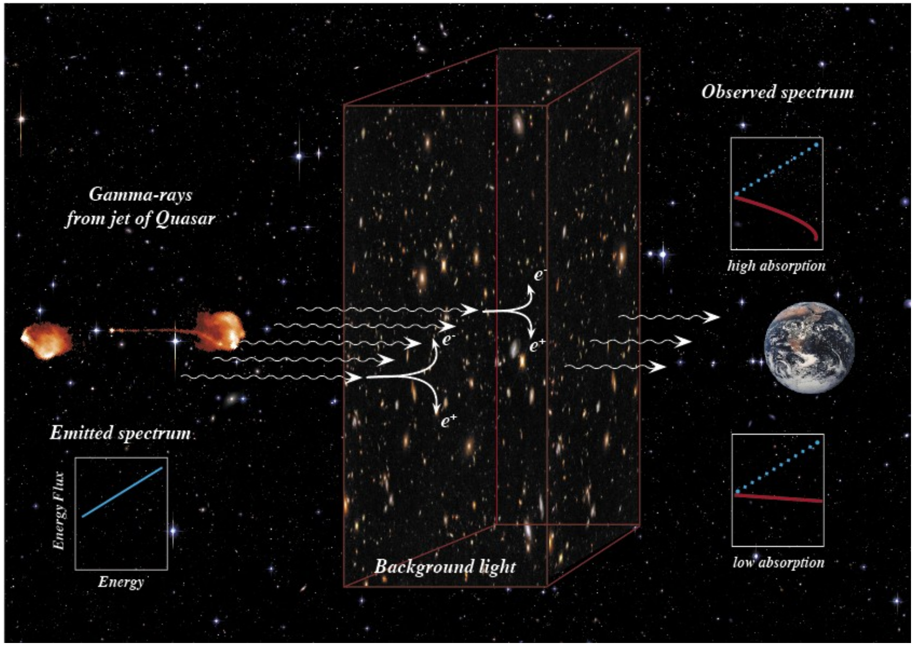

Spectra of distant objects are affected by the EBL absorption.

– spectra of 38 blazars analyzed (30 H.E.S.S. sources), 106 spectra

– total radiative content of the Universe 0.1-1000um: 6.5+/-1.2% of CMB brightness

Biteau & Williams 2015

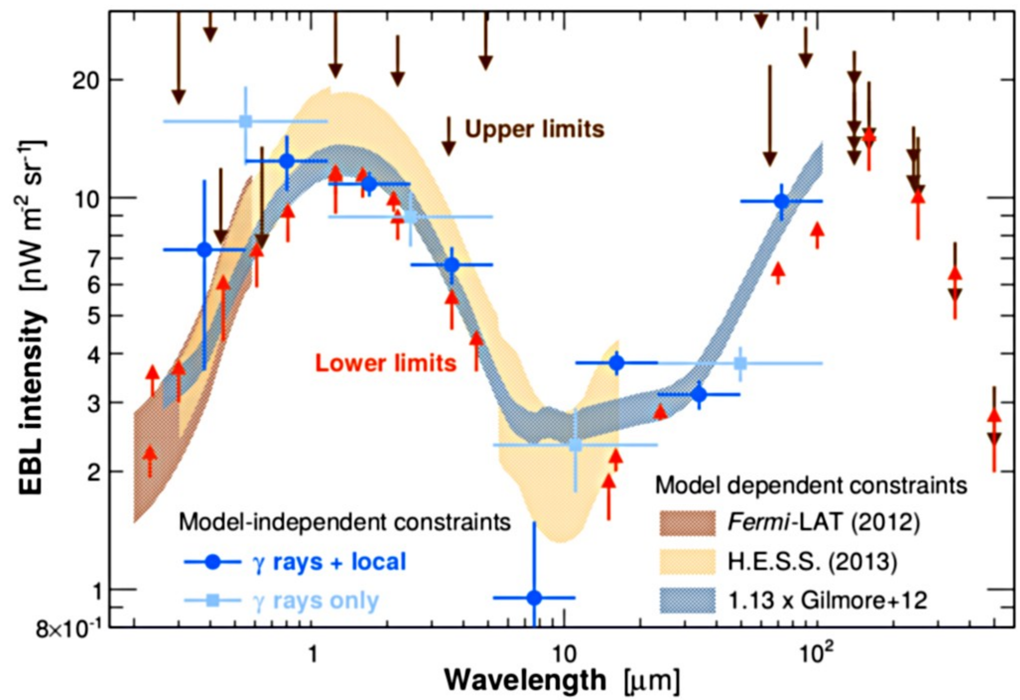

FIG. 3.— EBL intensity at $z = 0$ as a function of wavelength. The best-fit spectra derived in this work are shown with light blue (gamma rays only, four-point spectrum) and blue points (gamma rays + direct constraints, eight-point spectrum). Lower and upper limits are shown with orange upward-going and dark-brown downward-going arrows, respectively. For comparison with the work of Ackermann et al. (2012) and H.E.S.S. Collaboration (2013f), the 1σ (stat. + sys.) contour of the best-fit scaled-up model (Gilmore et al. 2012) is shown as filled blue region, using a scaling factor of 1.13 as shown in Table 4

Redshift determination

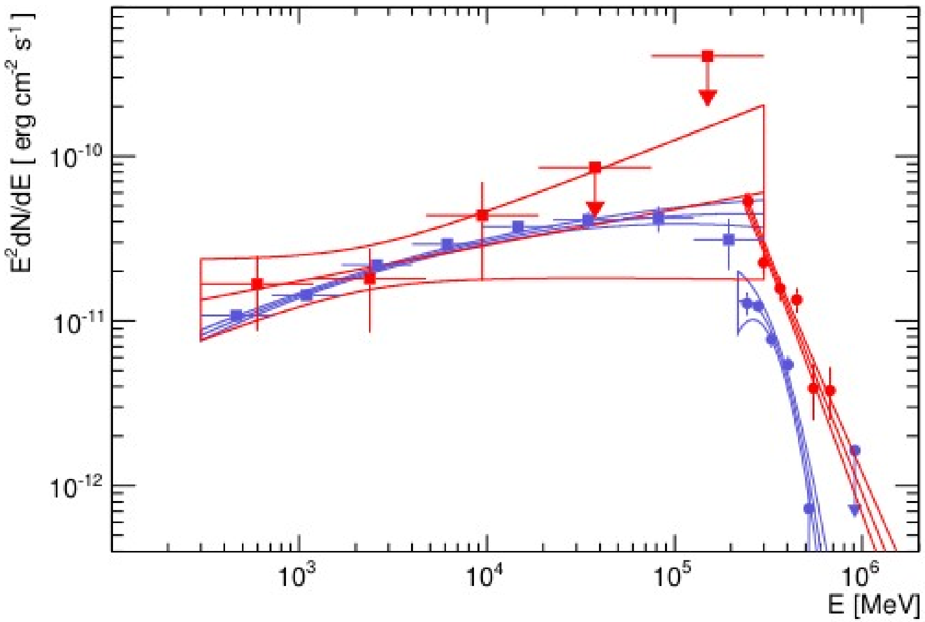

Fig. 3.— Spectral energy distribution of PG 1553+113 in γ-rays as measured by the *Fermi*-LAT and H.E.S.S. Red (resp blue) points and butterflies have been obtained during the flare (resp. pre-flare) period.

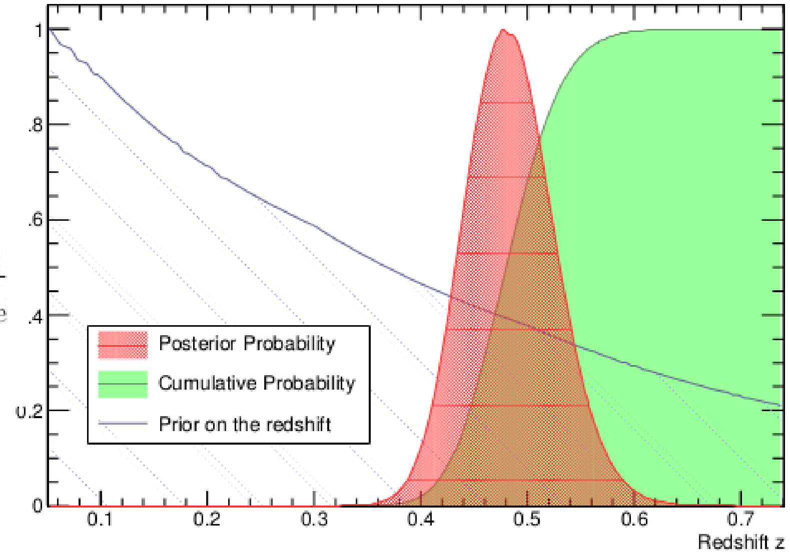

Fig. 6.— Posterior probability density as a function of the redshift (red). The green area represents the cumulative probability while the black line is the prior on z.

– for a source with unknown redshift a comparison of "extrapolated" spectrum with EBL absorbed observed spectrum may provide constraints on the source redshift

– for PG 1553+113 redshift has been determined to be z=0.49+/-0.04

Pair halos and magnetically broaden cascades

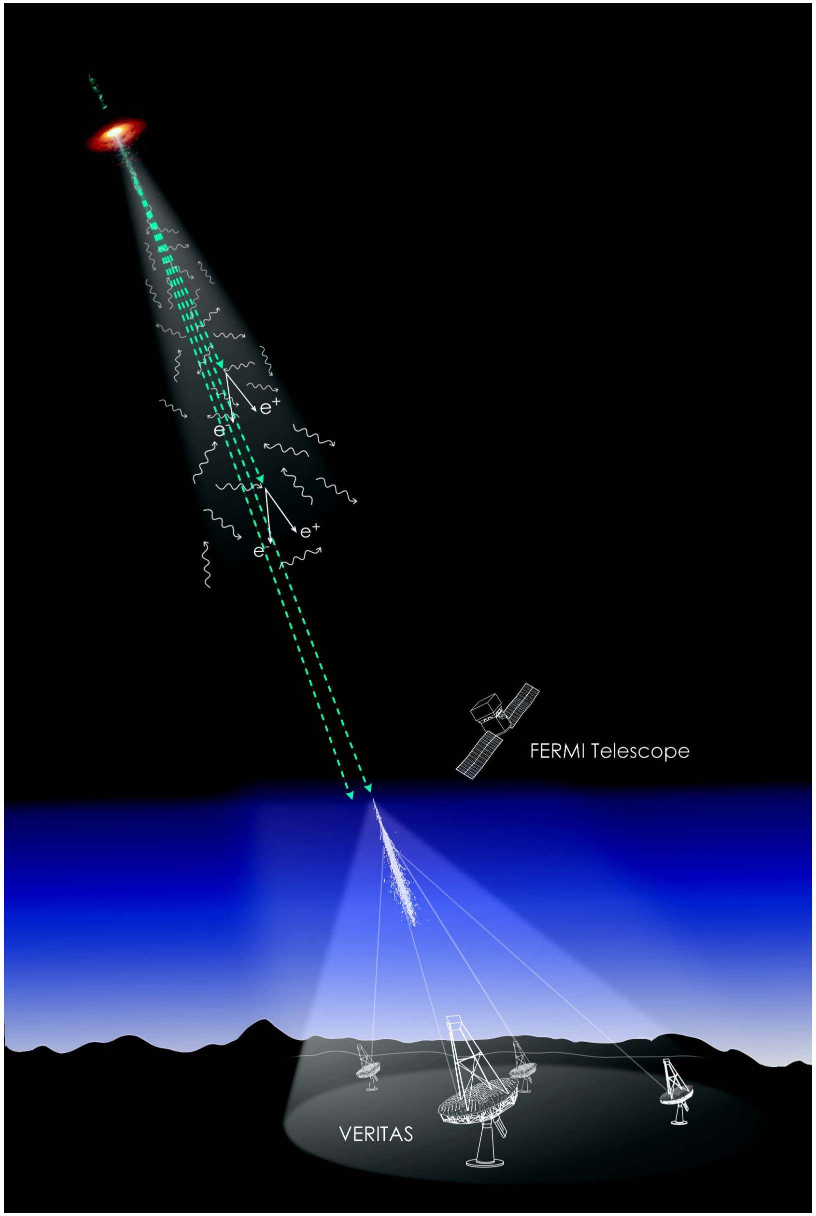

– three regimes:

I – strong magnetic field ($B>10^{-7}$G)

synchrotron cooling of e+-e- pairs prevents the production of secondary gamma-rays

II – intermediate magnetic field

pairs are isotropised and accumulate around the source, eventually giving raise to a **pair halo** (PH) of secondary gamma-rays

difficult to detect due to isotropic emission

III – weak magnetic field ($B<10^{-14}$G)

no pair halo, pair cascade continues to propagate along initial beam direction, broadened by deflection – **magnetically broaden cascade (MBC)**; transfer of energy between the electron and gamma-ray components

PH and MBC limits

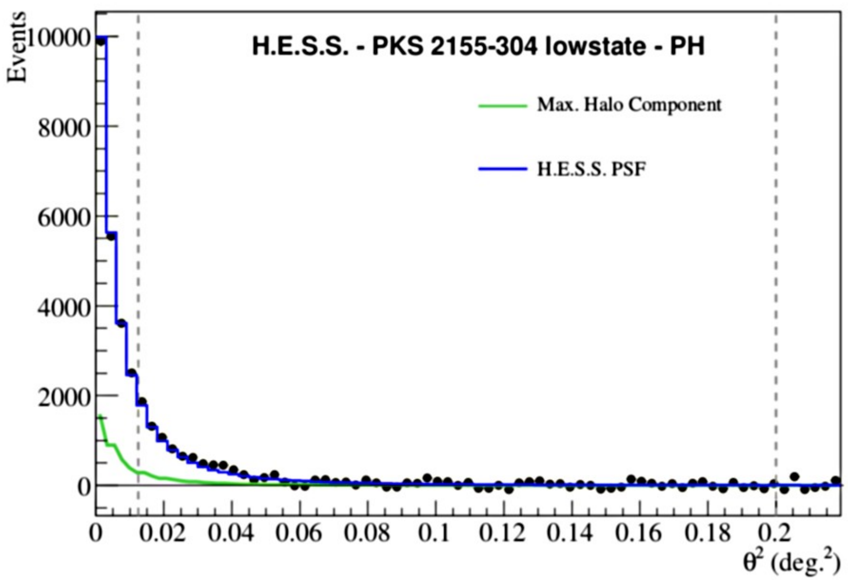

Fig. 2. Angular distribution of excess events of 1ES 1101-232 (top), 1ES 0229+200 (middle) and the PKS 2155-304 low state (bottom). The blue line is the H.E.S.S. PSF, the red line is the Halo Model scaled to the number of excess events and the green line is the maximum allowed halo component. The model independent limit on the pair halo excess is calculated between the vertical dashed lines at 0.0125 deg^2 and 0.02 deg^2.

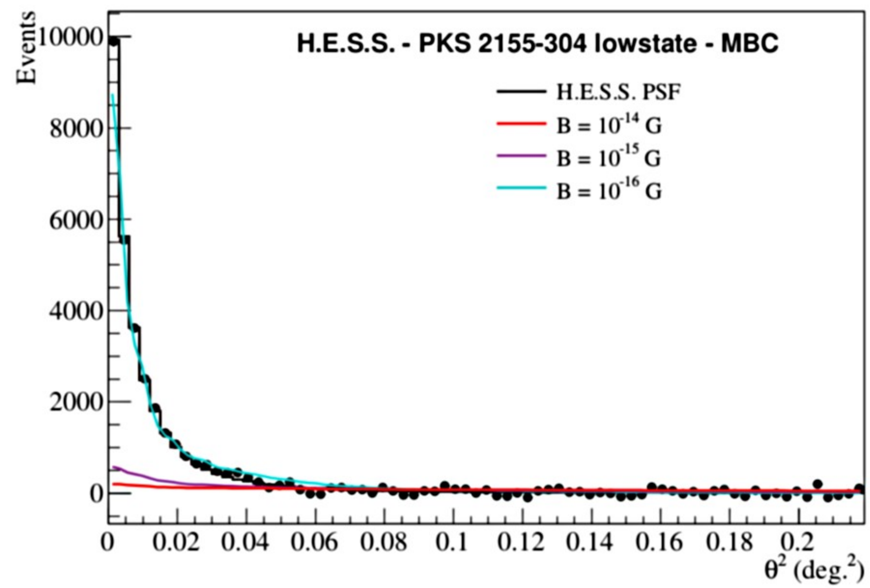

Fig. 4. Angular distribution of excess events of 1ES 1101-232 (top), 1ES 0229+200 (middle) and the PKS 2155-304 low state (bottom). The H.E.S.S. data (black points) is plotted against the angular distribution of the Magnetically Broadened Cascade Model for varying magnetic field strengths. The red, violet and cyan lines correspond to the simulated cascade flux for magnetic field strengths of 10^{-14}, 10^{-15} and 10^{-16} G.

PH and MBC limits

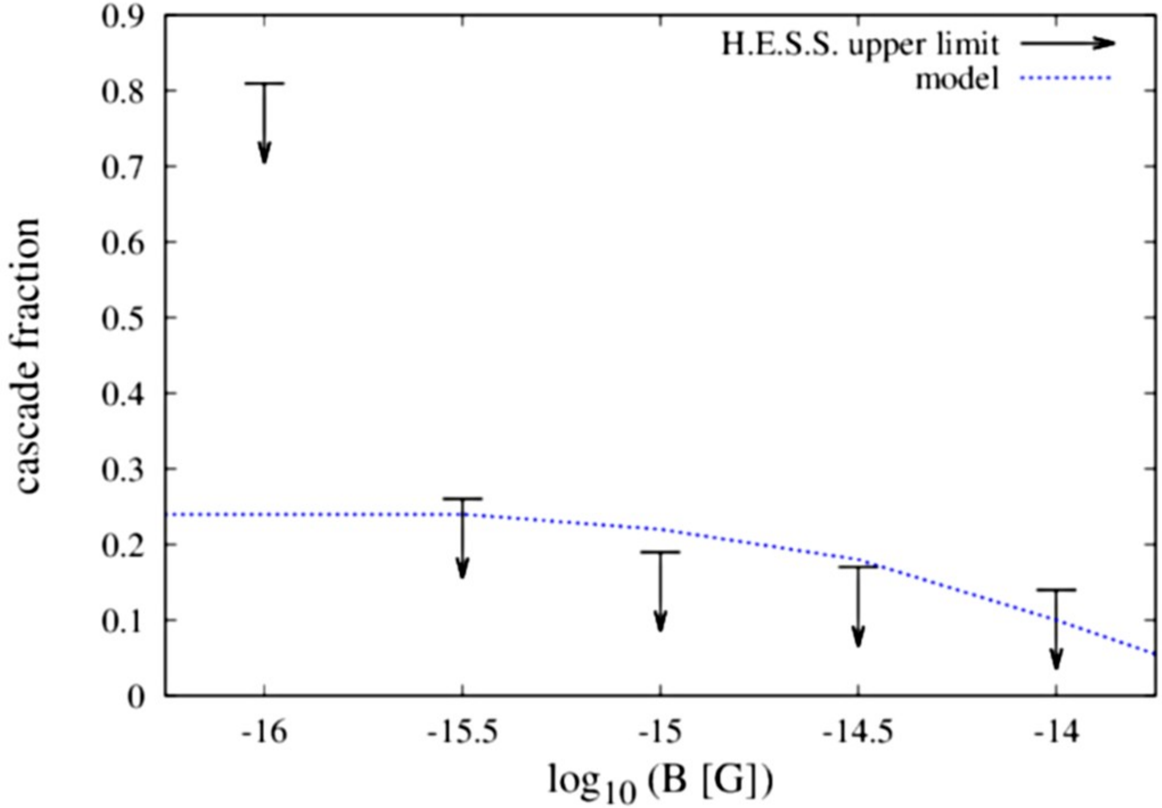

Fig. 6. EGMF constraints on PKS 2155-304. The blue dashed line depicts the expected fraction of MBC events in the VHE data depending on the EGMF strength. Black arrows are the maximum fractions of MBC events not contradicting the angular profile data of PKS 2155-304 at a 95% C.L.

Lorentz Invariance Violation (LIV)

– dispersion relation for light

$$c^2 p^2 = E^2 [1 \pm \xi (E/M) \pm \zeta (E/M)^2 \pm \ldots]$$

– high energy photons propagate faster (super-luminal) or slower (sub-luminal) than low energy photons
– dispersion parameter

$$\tau_n = \frac{\Delta t}{\Delta (E^n)} \simeq s_{\pm} \frac{(1+n)}{E_{QG}^n 2 H_0} \kappa_n$$

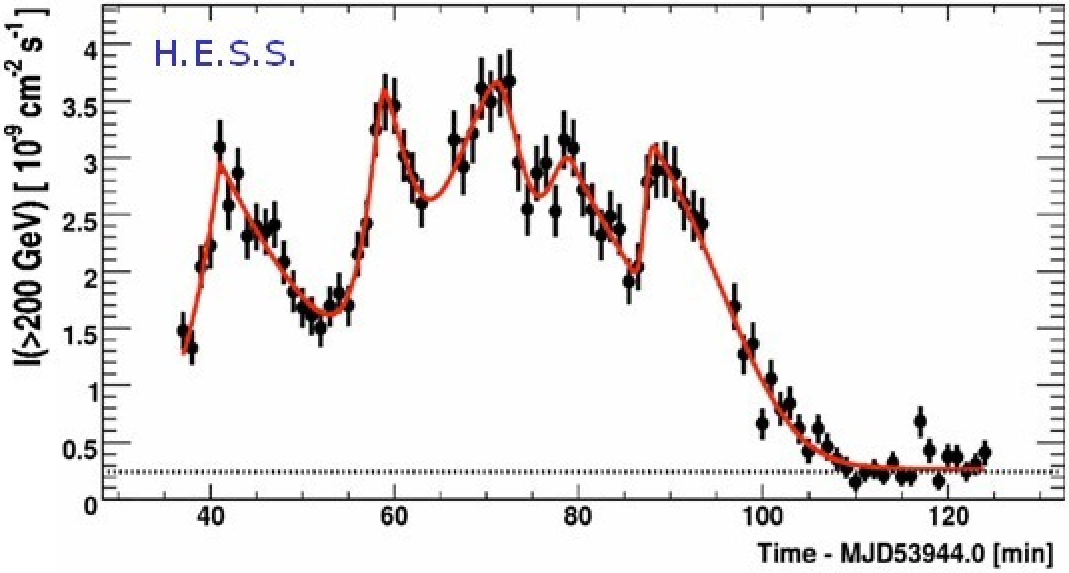

Lorentz Invariance Violation (LIV)

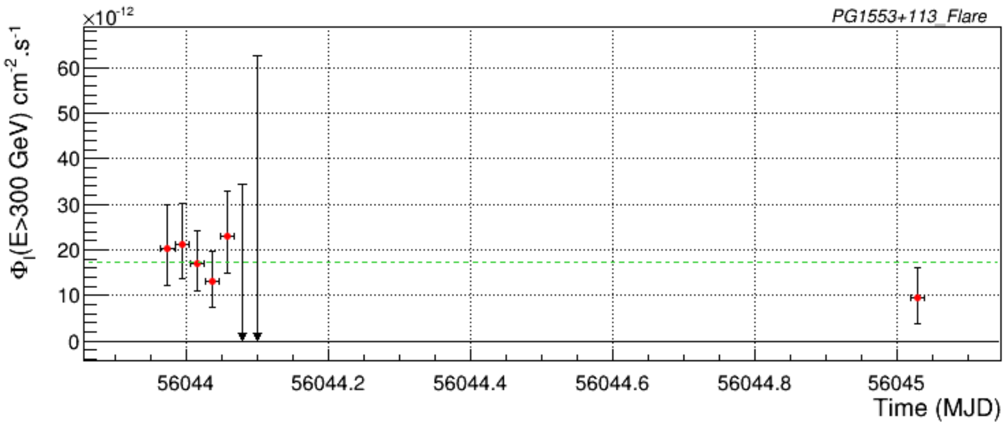

	Limits on τ_n (s.TeV^{-n})		Lower limits on E_{QG} (GeV)	
n	$LL^{calib+syst}$	$UL^{calib+syst}$	s = -1	s = +1
1	-799.8	537.4	2.90 10^{17}	4.32 10^{17}
2	-1530.9	973.4	1.68 10^{10}	2.11 10^{10}

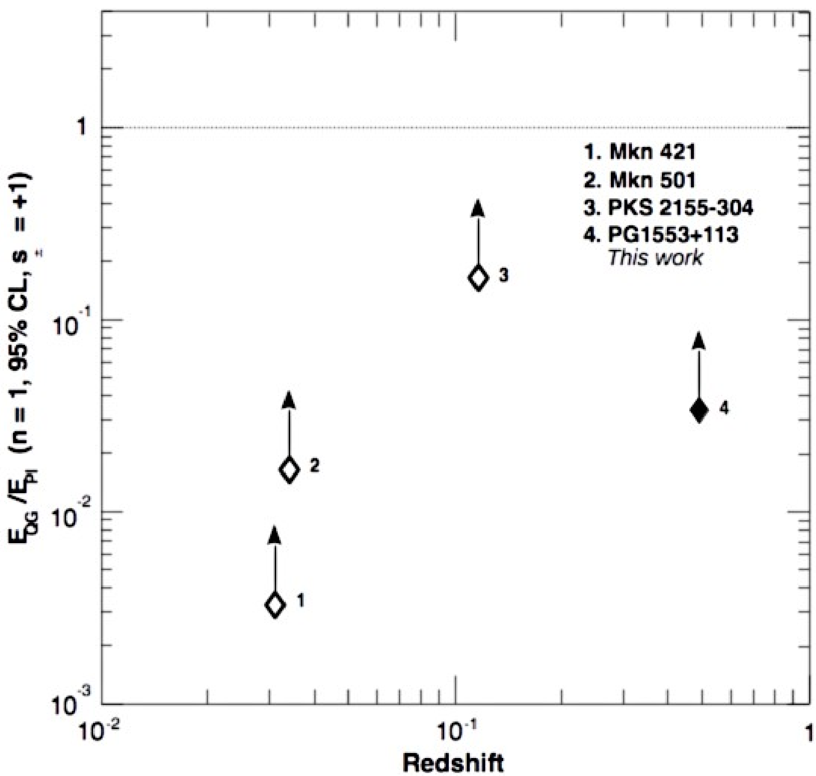

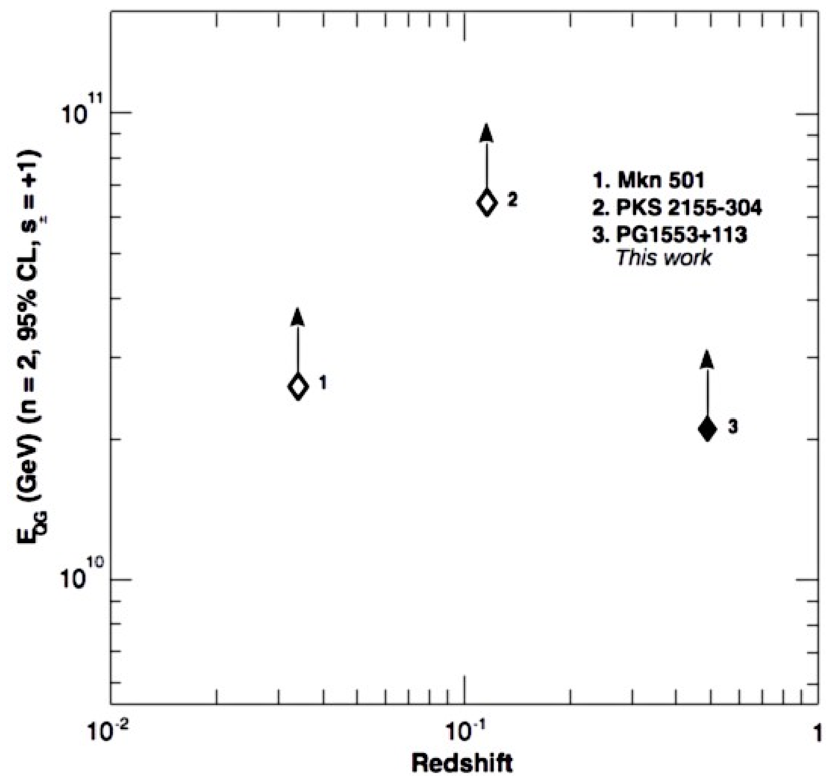

Gamma-ray Bursts (GRBs)

– peak at keV-MeV, but known to show emission >100MeV

– high energy emission delayed up to 40s and lasts longer (> 20h for GRB130427A)

– some predictions for very high energy (>100GeV) emission due to e.g. inverse Compton mechanism

– absorption on extragalactic background light limits observation horizon to z=0.6

GRB 100621A

– detected by Swift satellite, z=0.542 from VLT

– H.E.S.S. observations 683s after t_0

A&A 565, A16 (2014)

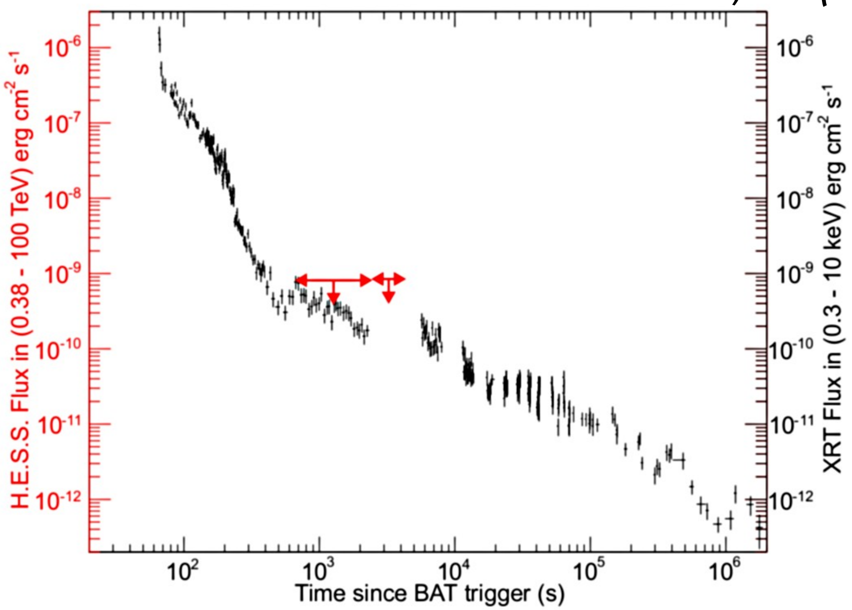

Fig. 2. Comparison of the VHE upper limits (95% confidence level) on the energy output above the energy threshold (in lighter colour) using the Band function extension model (no EBL correction applied) with the XRT energy flux (in darker colour, de-absorbed, from the Swift Burst Analyser, Evans et al. 2009, 2007). Horizontal arrows indicate the start and end time of the observations from which the corresponding upper limit is derived.

SUMMARY

– H.E.S.S. performs very well in many aspects of astroparticle research

– recent addition of CT5 telescope, mirror recoating and camera upgrade will allow for further improvement in performance

– H.E.S.S. is now a **hybrid system** – a pathfinder for the Cherenkov Telescope Array (CTA)